

# Small-Signal Amplification of Period-Doubling Bifurcations in Smooth Iterated Maps

Xiaopeng Zhao,<sup>1\*</sup> David G. Schaeffer,<sup>2</sup> Carolyn M. Berger,<sup>3</sup> and Daniel J. Gauthier,<sup>1,3</sup>  
 Department of <sup>1</sup>Biomedical Engineering, <sup>2</sup>Mathematics, and <sup>3</sup>Physics  
 and Center for Nonlinear and Complex Systems  
 Duke University, Durham, NC 27708

September 10, 2017

## Abstract

Various authors have shown that, near the onset of a period-doubling bifurcation, small perturbations in the control parameter may result in much larger disturbances in the response of the dynamical system. Such amplification of small signals can be measured by a gain defined as the magnitude of the disturbance in the response divided by the perturbation amplitude. In this paper, the perturbed response is studied using normal forms based on the most general assumptions of iterated maps. Such an analysis provides a theoretical footing for previous experimental and numerical observations, such as the failure of linear analysis and the saturation of the gain. Qualitative as well as quantitative features of the gain are exhibited using selected models of cardiac dynamics.

## 1 Introduction

We study a dynamical system described by a one-parameter family of iterated maps

$$x_{n+1} = f(x_n; \mu), \quad (1)$$

where the state  $x$  may be one- or multi-dimensional. Suppose that a fixed point of the map experiences a supercritical period-doubling bifurcation when the control parameter  $\mu$  passes through a critical value  $\mu_{\text{bif}}$ . Near onset of the bifurcation, the system is sensitive to small alternating perturbations applied to  $\mu$  [1-14]. Under such alternating perturbations, the governing map becomes

$$x_{n+1} = f(x_n; \mu + (-1)^n \delta), \quad (2)$$

where  $\delta$  is the perturbation amplitude. Consequently, the steady-state solution of the system alternates between two states,  $x_{\text{even}}$  and  $x_{\text{odd}}$ , in the following manner:

$$x_{\text{even}} = f(x_{\text{odd}}; \mu - \delta) \quad (3)$$

$$x_{\text{odd}} = f(x_{\text{even}}; \mu + \delta). \quad (4)$$

The magnitude of deviation between  $x_{\text{even}}$  and  $x_{\text{odd}}$  could be many times larger than the perturbation amplitude  $\delta$ , an effect which is known as pre-bifurcation amplification [7-9]. To characterize this amplification, one may define a gain using the  $i$ th component of  $x$  as follows

$$\Gamma \equiv \left| \frac{x_{\text{even}}^{(i)} - x_{\text{odd}}^{(i)}}{2\delta} \right|. \quad (5)$$

---

\*Corresponding author. Email: xzhao@duke.edu

In this work, we explore qualitative changes in the gain  $\Gamma$  under changes in the control parameter  $\mu$  and perturbation amplitude  $\delta$ .

It has been shown that pre-bifurcation amplification is a universal phenomenon existing in discrete [1-6] as well as continuous [7-10] dynamical systems. Many authors utilized one-dimensional maps to illustrate the scaling of parameters. Such one-dimensional maps either take the most general form as in Heldstab *et al.* [1] or take the normal form as in Bryant and Wiesenfeld [9]. Since the normal form in [9] was not related to the full-dimensional underlying model, it is not clear how the scaling of parameters is connected to physical properties of the system.

Although the fundamental scaling law behind prebifurcation amplification has been shown in the literature, explicit solutions of the gain  $\Gamma$  are not known for arbitrarily-given iterated maps. In this paper, we aim to derive an analytical formula of the gain based on multi-dimensional iterated maps, requiring only minimum assumptions. Using numerical simulations as well as experimental work [9, 11, 12], a few researchers have shown that the correct scaling law must resort to a nonlinear analysis. We illustrate, for the first time, the failure of the linear analysis through an order analysis, which reveals that the range of validity for the linear analysis is extremely limited and dramatically shrinks to zero as the bifurcation point is approached. We also explain the saturation of amplification previously observed in [13, 14] using the developed scaling law.

Another objective of the current work is to examine period-doubling bifurcations in cardiac dynamics, *i.e.*, alternans in cardiac tissues, which are characterized by the long-short beat-to-beat alternation in the duration of cardiac action potentials [15-18]. Cardiac alternans have been recognized as a possible initiator of fatal arrhythmia, which is the number one cause of death in the United States [19]. We apply the theoretical results to two cardiac mappings to help gain an understanding of the origin and control of instabilities in cardiac tissues.

The paper is organized as follows. In Section 2, we compute the response of alternating perturbations using linear analysis of the map. A nonlinear analysis based on higher-order approximation of the map is then performed in Section 3. A summary and discussion is presented in Section 4.

## 2 Linear Analysis

At  $\mu = \mu_{\text{bif}}$ , denote the fixed point of the map (1) by  $x_{\text{bif}}$ . Then the Jacobian  $f_x(x_{\text{bif}}; \mu_{\text{bif}})$  has one eigenvalue equal to  $-1$  with the corresponding right and left eigenvectors denoted by  $\phi_1$  and  $\psi_1$ , respectively. Near onset of the period-doubling bifurcation, the response of the perturbed map (2) exhibits pre-bifurcation amplification. The following theorem computes the amplification gain based on linearization of the perturbed map.

**Theorem 1.** *In linear approximation, as  $\mu \rightarrow \mu_{\text{bif}}$ , the gain defined in Eq. (5) diverges as*

$$\Gamma \sim \left| \frac{k}{\mu - \mu_{\text{bif}}} \right|, \quad (6)$$

where the constant  $k$  is determined by data from the mapping. Specifically,

$$k = \frac{\psi_1^T \cdot f_\mu(x_{\text{bif}}; \mu_{\text{bif}}) \phi_1^{(i)}}{(\psi_1^T \cdot L_1 \cdot \phi_1)}, \quad (7)$$

where

$$L_1 = f_{xx}(x_{\text{bif}}; \mu_{\text{bif}}) \cdot \frac{\partial x_*}{\partial \mu}(\mu_{\text{bif}}) + f_{x\mu}(x_{\text{bif}}; \mu_{\text{bif}}), \quad (8)$$

and  $x_*(\mu)$  is a fixed point of map (1).

In Theorem 1,  $\phi_1^{(i)}$  represents the  $i$ th component of  $\phi_1$ . For one-dimensional maps, the eigenvectors are  $\phi_1 = \psi_1 = 1$  and thus

$$k = \frac{f_\mu(x_{\text{bif}}; \mu_{\text{bif}})}{f_{xx}(x_{\text{bif}}; \mu_{\text{bif}}) \cdot \frac{\partial x_*}{\partial \mu}(\mu_{\text{bif}}) + f_{x\mu}(x_{\text{bif}}; \mu_{\text{bif}})}. \quad (9)$$

Note, here, subscripts indicate partial derivatives of the function  $f$ . This theorem indicates that the magnitude of the gain depends on the properties of the system at the bifurcation point. Moreover, one can make two striking observations regarding the linear approximation: i) the gain does not depend on the amplitude  $\delta$  and ii) the gain approaches  $\infty$  as  $\mu \rightarrow \mu_{\text{bif}}$ . As shown at the end of this section, both observations compare poorly with numerical simulations. To rectify the discrepancy, we are led to the higher-order nonlinear analysis of the gain in Section 3.

## 2.1 Proof of Theorem 1

We prove the theorem by a perturbation-theory calculation. We assume the map (1) is  $N$ -dimensional. Denote the fixed point of map (1) as  $x_*(\mu)$ , so that

$$x_*(\mu) = f(x_*(\mu); \mu). \quad (10)$$

Let us assume the fixed point is stable when  $\mu$  is greater than but close to  $\mu_{\text{bif}}$  (otherwise we could introduce a new control parameter as  $\bar{\mu} = -\mu$ ). We then study the response of the perturbed map (2). Under small perturbation, the response of the perturbed system is a small deviation (denoted by  $d_n$ ) from the unperturbed fixed point. Let us write  $x_n = x_* + d_n$ , which upon substitution into Eq. (2), yields

$$d_{n+1} = L \cdot d_n + (-1)^n f_\mu(x_*; \mu) \delta, \quad (11)$$

where

$$L = f_x(x_*; \mu). \quad (12)$$

To account for the alternating feature of the perturbation, we decompose the steady state of  $d_n$  into an oscillating component  $(-1)^n v$  and a mean value  $m$ : *i.e.*,  $d_n = (-1)^n v + m$ . Substituting  $d_n$  into Eq. (11) yields

$$m = L \cdot m \quad (13)$$

$$v = -L \cdot v - f_\mu(x_*; \mu) \delta. \quad (14)$$

It follows that  $m = 0$  in this linear approximation.

In the following, we find a solution for  $v$ . Because  $\mu$  is close to  $\mu_{\text{bif}}$ ,  $L$  can be approximated as

$$L = L_0 + (\mu - \mu_{\text{bif}}) L_1, \quad (15)$$

where

$$L_0 = f_x(x_{\text{bif}}; \mu_{\text{bif}}) \quad (16)$$

$$L_1 = f_{xx}(x_{\text{bif}}; \mu_{\text{bif}}) \cdot \frac{\partial x_*}{\partial \mu}(\mu_{\text{bif}}) + f_{x\mu}(x_{\text{bif}}; \mu_{\text{bif}}). \quad (17)$$

Implicit differentiation of Eq. (10) yields

$$\frac{\partial x_*}{\partial \mu}(\mu_{\text{bif}}) = (\mathbf{I} - f_x(x_{\text{bif}}; \mu_{\text{bif}}))^{-1} \cdot f_\mu(x_{\text{bif}}; \mu_{\text{bif}}), \quad (18)$$

where  $\mathbf{I}$  stands for the identity matrix. Denote the eigenvalues of  $L_0$  by  $-1 = \lambda_1 < \lambda_2 \leq \dots \leq \lambda_N < 1$  and denote the corresponding right and left eigenvectors by  $\phi_1, \phi_2, \dots, \phi_N$  and  $\psi_1^T, \psi_2^T, \dots, \psi_N^T$ , respectively. Assume the eigenvectors are normalized such that  $\psi_i^T \cdot \phi_j = 1$  if  $i = j$  and  $\psi_i^T \cdot \phi_j = 0$  if  $i \neq j$ . We can decompose  $v$  as

$$v = \sum_{i=1}^N s_i \phi_i. \quad (19)$$

Substituting Eq. (19) into Eq. (14) yields

$$\sum_{i=1}^N (\mathbf{I} + L_0) \cdot \phi_i s_i + (\mu - \mu_{\text{bif}}) \sum_{i=1}^N L_1 \cdot \phi_i s_i = -f_\mu(x_*; \mu) \delta. \quad (20)$$

The dot product on both sides of Eq. (20) with  $\psi_j^T$  for  $j = 1, \dots, N$  yields

$$(1 + \lambda_j) s_j + (\mu - \mu_{\text{bif}}) \sum_{i=1}^N \psi_j^T \cdot L_1 \cdot \phi_i s_i = -\psi_j^T \cdot f_\mu(x; \mu) \delta. \quad (21)$$

Because  $1 + \lambda_1 = 0$ , it follows that  $s_2, \dots, s_N$  are negligible compared to  $s_1$ . To lowest order, solution of  $s_1$  is

$$s_1 = -\frac{\psi_1^T \cdot f_\mu(x; \mu)}{(\mu - \mu_{\text{bif}}) (\psi_1^T \cdot L_1 \cdot \phi_1)} \delta. \quad (22)$$

Thus, an approximation of  $v$  is

$$v = -\frac{\psi_1^T \cdot f_\mu(x; \mu)}{(\mu - \mu_{\text{bif}}) (\psi_1^T \cdot L_1 \cdot \phi_1)} \phi_1 \delta. \quad (23)$$

In steady state, the solution of the perturbed system alternates between two states,  $x_{\text{even}}$  and  $x_{\text{odd}}$ , where

$$x_{\text{even}} = x_* + v, \quad (24)$$

$$x_{\text{odd}} = x_* - v. \quad (25)$$

Recalling definition (5) of the gain yields

$$\Gamma = \left| \frac{v^{(i)}}{\delta} \right| \sim \left| \frac{k}{\mu - \mu_{\text{bif}}} \right|, \quad (26)$$

where

$$k = \frac{\psi_1^T \cdot f_\mu(x_{\text{bif}}; \mu_{\text{bif}})}{\psi_1^T \cdot L_1 \cdot \phi_1} \phi_1^{(i)}. \quad (27)$$

## 2.2 An Example Illustrating the Limitation of the Linear Analysis

As the first numerical example, we consider a one-dimensional cardiac map [16]:

$$A_{n+1} = A_{\text{max}} - \alpha e^{-D_n/\tau} \quad (28)$$

where  $D_n = B - A_n$ . Here,  $A_n$  is the  $n$ th duration of action potential of a cardiac cell under an electrical pacing with period  $B$  (known as the basic cycle length);  $D_n$  is the  $n$ th diastolic interval. Using the parameters  $A_{\text{max}} = 392.0$  ms,  $\alpha = 525.3$  ms, and  $\tau = 40.0$  ms, Hall and Gauthier [16] showed that a period-doubling bifurcation occurs at  $B = B_{\text{bif}} \approx 455$  ms and the period-one fixed point of the system is stable for  $B > B_{\text{bif}}$ . We refer interested readers to [16] for a bifurcation diagram exhibiting the period-doubling bifurcation and other properties of this map.

It is our interest to study the response of this cardiac map when the basic cycle length  $B$  is perturbed with an alternating perturbation in such a way that  $D_n = B + (-1)^n \delta - A_n$ . Following Theorem 1 and evaluating the corresponding derivatives, one obtains the amplification gain as

$$\Gamma \sim \frac{2\tau}{B - B_{\text{bif}}}. \quad (29)$$

Again, the theorem predicts i) the gain does not depend on perturbation amplitude  $\delta$  and ii) the gain approaches  $\infty$  when the control parameter  $B \rightarrow B_{\text{bif}}$ . For a given  $B$ , the magnitude of the gain depends on the value of the parameter  $\tau$ . To verify these observations, we compare results from theory and numerical simulations, as shown in Fig. 1. Here, Fig. 1 (a) shows variation of the gain under changes in the control parameter  $B$  when the perturbation amplitude  $\delta$  takes on various constant values and Fig. 1 (b) shows variation of the gain under changes in  $\delta$  when  $B$  takes on various constant values. In both figures, numerical simulations indicate that the gain strongly depends on  $\delta$ . It is also noted that the gain is not  $\infty$  at  $B = B_{\text{bif}}$  except when  $\delta = 0$ . These qualitative differences between the linear analysis and numerical simulations therefore demand a higher-order nonlinear analysis of the gain, which will be presented in the following section.

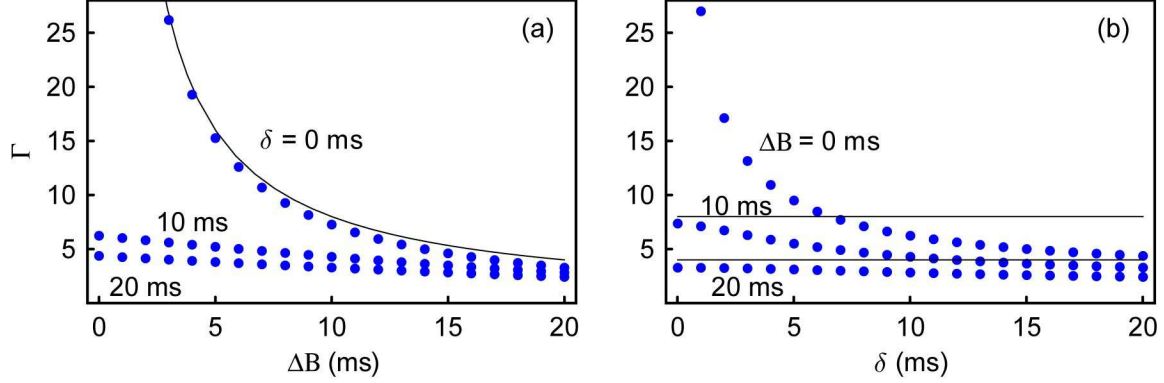


Figure 1: Variation of the gain for the 1-D cardiac map as function of (a)  $\Delta B = B - B_{\text{bif}}$  and (b) perturbation amplitude  $\delta$ : the solid curves correspond to results from the linear analysis and the dots correspond to numerical simulations. Note that, in (b), the linear analysis predicts an infinitely large gain for  $\Delta B = 0$  and any  $\delta$ .

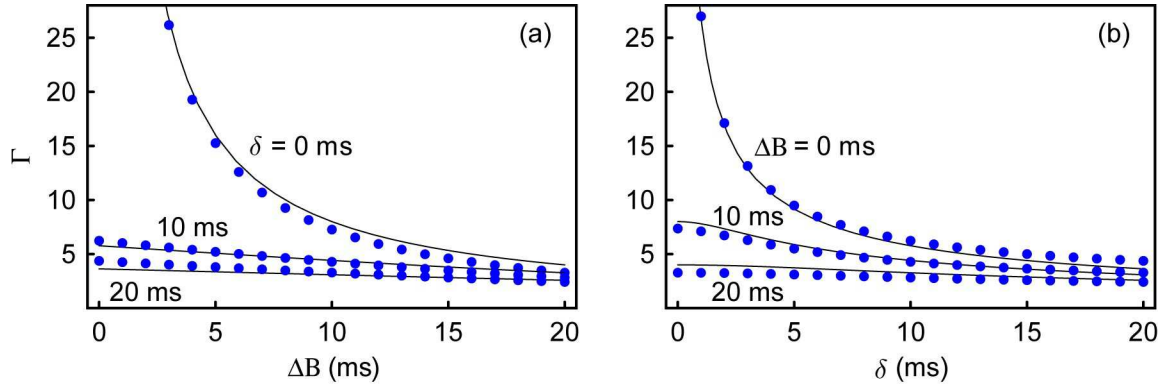


Figure 2: Variation of gain for the 1-D cardiac map as function of (a)  $\Delta B = B - B_{\text{bif}}$  and (b) perturbation amplitude  $\delta$ : the solid curves correspond to results from the higher-order nonlinear analysis and the dots correspond to numerical simulations.

### 3 Higher-Order Analysis

Again, denote the fixed point of the map (1) at  $\mu = \mu_{\text{bif}}$  by  $x_{\text{bif}}$ . And again, denote by  $\phi_1$  and  $\psi_1$  the right and left eigenvectors associated with the  $-1$  eigenvalue of the Jacobian  $f_x(x_{\text{bif}}; \mu_{\text{bif}})$ . Near onset of the period-doubling bifurcation, the response of the perturbed map (2) exhibits pre-bifurcation amplification. The following theorem computes the amplification gain based on a higher-order nonlinear analysis of the perturbed map.

**Theorem 2.** *To leading order, the gain defined in Eq. (5) satisfies the following relation,*

$$c \delta^2 \Gamma^3 + (\mu - \mu_{\text{bif}}) \Gamma - |k| = 0. \quad (30)$$

*The coefficients in Eq. (30) are defined in the following subsection.*

Here, again,  $\phi_1^{(i)}$  represents the  $i$ th component of  $\phi_1$ . For the special case of one-dimensional maps, the

eigenvectors are  $\phi_1 = \psi_1 = 1$  and thus

$$k = \frac{f_\mu(x_{\text{bif}}; \mu_{\text{bif}})}{f_{xx}(x_{\text{bif}}; \mu_{\text{bif}}) \cdot \frac{\partial x_*}{\partial \mu}(\mu_{\text{bif}}) + f_{x\mu}(x_{\text{bif}}; \mu_{\text{bif}})} \quad (31)$$

$$c = \frac{(1/2 f_{xx}(x_{\text{bif}}; \mu_{\text{bif}}))^2 + 1/6 f_{xxx}(x_{\text{bif}}; \mu_{\text{bif}})}{f_{xx}(x_{\text{bif}}; \mu_{\text{bif}}) \cdot \frac{\partial x_*}{\partial \mu}(\mu_{\text{bif}}) + f_{x\mu}(x_{\text{bif}}; \mu_{\text{bif}})}. \quad (32)$$

Theorem 2 clearly indicates that the gain strongly depends on  $\delta$  as well as  $\mu$ . Especially at the bifurcation point, where  $\mu = \mu_{\text{bif}}$ , the gain approaches to  $\infty$  as a function  $\delta^{-2/3}$ . As shown by numerical examples at the end of this section, the higher-order analysis agrees well with numerical simulations.

### 3.1 Proof of Theorem 2

Heldstab *et al.* [1] seemingly were the first to conduct a higher-order nonlinear analysis of the perturbed map (2). Letting  $\mu = \mu_{\text{bif}}$ , they calculated the response of alternating perturbations in one-dimensional maps. It was shown that deviation between  $x_{\text{even}}$  and  $x_{\text{odd}}$  is proportional to  $\delta^{1/3}$ . Following the same line of approach, we study the nonlinear response of maps of any dimensions and consider the influence of both the control parameter  $\mu$  and the perturbation amplitude  $\delta$ . Naturally, the first attempt of higher-order analysis is to include only quadratic terms, which, as shown in the following, modifies the expressions for the median of the response as well as modulates its amplitude. A retrospective examination reveals that the contribution to the response from the cubic term is comparable to that from the quadratic term and thus the cubic term has to be taken into account.

Again, we assume the perturbed response is a deviation  $d_n$  away from the unperturbed response  $x_*$ , defined in Eq. (10). Substituting  $x_n = x_* + d_n$  into Eq. (2) and keeping the expansion of  $f$  up to cubic order in  $d_n$  yields

$$d_{n+1} = L \cdot d_n + Q \cdot d_n \cdot d_n + C \cdot d_n \cdot d_n \cdot d_n + (-1)^n f_\mu(x; \mu) \delta + \dots, \quad (33)$$

where

$$L = f_x(x; \mu) \quad (34)$$

$$Q = \frac{1}{2} f_{xx}(x; \mu) \quad (34)$$

$$C = \frac{1}{6} f_{xxx}(x; \mu). \quad (35)$$

To account for the alternating feature of the perturbation, we decompose the steady state of  $d_n$  into an oscillating component  $(-1)^n v$  and a mean value  $m$ . Substituting  $d_n = (-1)^n v + m$  into Eq. (33) yields

$$m = L \cdot m + Q \cdot v \cdot v \quad (36)$$

$$v = -L \cdot v - 2Q \cdot m \cdot v - C \cdot v \cdot v \cdot v - f_\mu(x; \mu) \delta. \quad (37)$$

Because  $\mu$  is close to  $\mu_{\text{bif}}$ ,  $L$  can be approximated as

$$L = L_0 + (\mu - \mu_{\text{bif}}) L_1, \quad (38)$$

where  $L_0$  and  $L_1$  are defined in Eqs. (16) and (17). Again, denote the eigenvalues of  $L_0$  by  $-1 = \lambda_1 < \lambda_2 \leq \dots \leq \lambda_N < 1$  and denote the corresponding right and left eigenvectors by  $\phi_1, \phi_2, \dots, \phi_N$  and  $\psi_1^T, \psi_2^T, \dots, \psi_N^T$ , respectively. We assume the eigenvectors are normalized such that  $\psi_i^T \cdot \phi_j = 1$  if  $i = j$  and  $\psi_i^T \cdot \phi_j = 0$  if  $i \neq j$ .

It follows from Eq. (36) that, in steady state,

$$m = \tilde{Q} \cdot v \cdot v, \quad (39)$$

where

$$\tilde{Q} = (\mathbf{I} - L_0)^{-1} \cdot Q. \quad (40)$$

To solve for the steady-state solution of  $v$ , we again decompose  $v$  as

$$v = \sum_{i=1}^N s_i \phi_i = \Phi \cdot s, \quad (41)$$

where  $\Phi = (\phi_1, \dots, \phi_N)$  and  $s = (s_1, \dots, s_N)^T$ . Substituting Eq. (41) into Eq. (37) and taking the dot-product of this expression with  $\psi_j$  for  $j = 1, \dots, N$  on both sides yields

$$(1 + \lambda_j) s_j + (\mu - \mu_{\text{bif}}) \sum_{i=1}^N \psi_j^T \cdot L_1 \cdot \phi_i s_i \quad (42)$$

$$= -2\psi_j^T \cdot Q \cdot \left( \tilde{Q} \cdot (\Phi \cdot s) \cdot (\Phi \cdot s) \right) \cdot (\Phi \cdot s) \quad (43)$$

$$- \psi_j^T \cdot C \cdot (\Phi \cdot s) \cdot (\Phi \cdot s) \cdot (\Phi \cdot s) - \psi_j^T \cdot f_\mu(x; \mu) \delta. \quad (44)$$

Because  $1 + \lambda_1 = 0$ , it follows that  $s_2, \dots, s_N$  are higher order compared to  $s_1$  and thus  $v \approx \phi_1 s_1$ . Then, the governing equation for  $s_1$  is, to lowest order,

$$(\bar{Q} + \bar{C}) s_1^3 + (\mu - \mu_{\text{bif}}) \bar{L} s_1 + \psi_1^T \cdot f_\mu(x; \mu) \delta = 0, \quad (45)$$

where

$$\bar{L} = \psi_1^T \cdot L_1 \cdot \phi_1 \quad (46)$$

$$\bar{Q} = 2\psi_1^T \cdot Q \cdot \left( \tilde{Q} \cdot \phi_1 \cdot \phi_1 \right) \cdot \phi_1 \quad (47)$$

$$\bar{C} = \psi_1^T \cdot C \cdot \phi_1 \cdot \phi_1 \cdot \phi_1. \quad (48)$$

The perturbed response governed by Eq. (45) is valid for both supercritical and subcritical period-doubling bifurcations. However, for a supercritical period-doubling bifurcation such as the one mediating cardiac alternans,  $s_1 = 0$  is the only solution when  $\delta = 0$  and  $\mu > \mu_{\text{bif}}$ ; that is to say, before the occurrence of a supercritical period-doubling bifurcation, the only solution of the unperturbed map (1) is the period-one solution. Thus, for a supercritical period-doubling bifurcation, it follows from Eq. (45) that

$$(\bar{Q} + \bar{C}) \bar{L} > 0. \quad (49)$$

In the following, we restrict our attention to supercritical period-doubling bifurcations to simplify the result.

In steady state, the solution of the perturbed system alternates between two states,  $x_{\text{even}}$  and  $x_{\text{odd}}$ , where

$$x_{\text{even}} = x_* + v. \quad (50)$$

$$x_{\text{odd}} = x_* - v. \quad (51)$$

Recalling the definition of the gain yields

$$\Gamma = \left| \frac{\phi_1^{(i)} s_1}{\delta} \right|. \quad (52)$$

Substituting Eq. (52) into (45) yields

$$c \delta^2 \Gamma^3 + (\mu - \mu_{\text{bif}}) \Gamma - |k| = 0, \quad (53)$$

where

$$c = \frac{\bar{Q} + \bar{C}}{\bar{L} \left( \phi_1^{(i)} \right)^2}, \quad (54)$$

and  $k$  is defined in Eq. (27).

## 3.2 Examples Applying the Nonlinear Analysis

### 3.2.1 One-Dimensional Cardiac Model

Using the higher-order analysis, we reexamine the one-dimensional cardiac model described by Eq. (28). Results from the higher-order analysis agree well with numerical simulations, as seen in Fig. 2. It is observed from Eq. (53), as well as the numerical results, that the gain has a strong dependence on  $\delta$  and the gain in general is not  $\infty$  at  $B = B_{\text{bif}}$  except when  $\delta = 0$ . The discrepancy between the linear and nonlinear analyses can be seen clearer in Fig. 3, which shows the error between the linear and nonlinear predictions in two-dimensional parameter space  $(\Delta B, \delta)$ . The figure shows that the error increases as  $\delta$  increases and for the same  $\delta$  the error decreases as  $\Delta B$  increases.

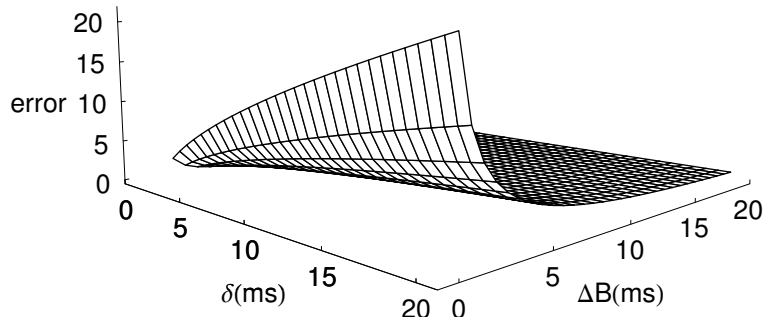


Figure 3: Discrepancy between the linear and nonlinear analyses for the the 1-D cardiac map. Here, the error is defined as  $(\Gamma_L - \Gamma_N) / \Gamma_N$ , where  $\Gamma_L$  is the result from the linear analysis and  $\Gamma_N$  is the result from the nonlinear analysis.

### 3.2.2 Two-Dimensional Cardiac Model

We now consider a two-dimensional map presented by Chialvo *et al.* [15] and later studied by Hall and Gauthier [16]

$$A_{n+1} = (1 - M_{n+1}) (A_{\max} - \alpha e^{-D_n/\tau}), \quad (55)$$

$$M_{n+1} = [1 - (1 - M_n)e^{-A_n/\tau_2}]e^{-D_n/\tau_2}, \quad (56)$$

where  $D_n = B - A_n$ ,  $A_n$  is the  $n$ th duration of action potential of a cardiac cell,  $B$  is the basic cycle length representing the period of applied electrical pacing, and  $D_n$  is the  $n$ th diastolic interval. Using the parameters  $A_{\max} = 490.9$  ms,  $\alpha = 569.0$  ms,  $\tau_1 = 64.0$  ms,  $\tau_2 = 38.0$  ms,  $D_{\min} = 38.0$  ms, Hall and Gauthier showed that a transition to alternans occurs at  $B = B_{\text{bif}} \approx 455$  ms [16]. We refer interested readers to [16] for a bifurcation diagram exhibiting the period-doubling bifurcation and other properties of this map. We study the response of this map under alternating perturbations. Figure 4 shows the variation of the amplification gain under changes in  $B$  and  $\delta$ . Again, it is seen that good agreement is achieved between the higher-order analysis and the numerical simulations.

## 4 Conclusion and Discussion

Using both linear and higher-order analyses, we have investigated the pre-bifurcation amplification near a period-doubling bifurcation in multi-dimensional iterated maps. Through numerical examples, it has been established that the qualitative features of the amplification gain can only be captured using the higher-order analysis. In general, the gain is a nonlinear function of  $\mu$  and  $\delta$  as seen from Eq. (53). In the  $(\mu, \delta)$  parameter region, the gain is finite everywhere except at  $(\mu_{\text{bif}}, 0)$ . Moreover, the rate of divergence as  $(\mu, \delta)$  approaches to this singular point depends on the path taken. Under two situations, this nonlinear function



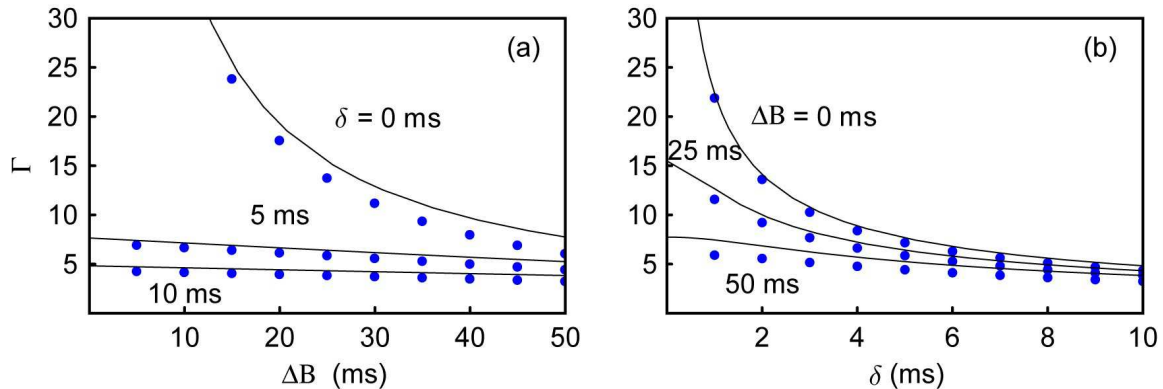


Figure 4: Variation of the gain for the two-dimensional cardiac map as function of (a)  $\Delta B = B - B_{\text{bif}}$  and (b) perturbation amplitude  $\delta$ : the solid curves correspond to results from the higher-order nonlinear analysis and the dots correspond to numerical simulations.

can be significantly simplified. First, when  $|\mu - \mu_{\text{bif}}| \gg \delta^{2/3}$ , the first term in Eq. (53) becomes negligible compared to the others, resulting in the simplified expression

$$(\mu - \mu_{\text{bif}}) \Gamma - |k| = 0. \quad (57)$$

It follows that the gain can be approximated by

$$\Gamma = \left| \frac{k}{\mu - \mu_{\text{bif}}} \right|, \quad (58)$$

which is the result of linear analysis obtained in Section 2. On the other hand, when  $|\mu - \mu_{\text{bif}}| \ll \delta^{2/3}$ , the

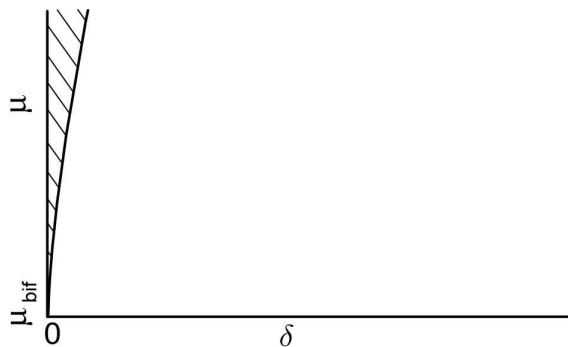


Figure 5: Range of validity: the linear analysis is valid in the hatched area; the higher-order analysis is valid in the whole region. Here, it has been assumed that region of interest is when  $\mu > \mu_{\text{bif}}$ .

second term in Eq. (53) becomes negligible compared to the others, resulting in the simplified expression

$$c \delta^2 \Gamma^3 - |k| = 0. \quad (59)$$

It follows that the gain can be approximated by

$$\Gamma = \sqrt[3]{\left| \frac{k}{c} \right|} \delta^{-2/3}. \quad (60)$$

A special case of the latter situation is when  $\mu = \mu_{\text{bif}}$ , which was studied by Heldstab *et al.* using one-dimensional maps [1]. Note that Heldstab *et al.* did not include the contribution due to the cubic order

expansion of  $v$  (*i.e.* the contribution of  $C$ ), although their result is still valid for the logistic map because  $C = 0$  for this map. Our analysis allows us to predict the range of validity for the linear and the higher-order analyses, as shown in Fig. 5. Especially, the linear analysis is only valid in a restricted area, which shrinks to zero as  $\mu$  approaches  $\mu_{\text{bif}}$ , cf. the numerical illustration in Fig. 3.

The two aforementioned special situations and the analysis of the range of validity lead to an interesting observation on the relationship between the gain  $\Gamma$  and the parameters. First, when  $\delta$  takes on a constant value, one can see from Figure 6 (a) that  $\log \Gamma$  is almost proportional to  $\log(\mu - \mu_{\text{bif}})^{-1}$  for large  $\mu$ , and  $\log \Gamma$  increases and saturates to a constant as  $\mu$  decreases to a sufficiently small value. Conversely, when  $\mu$  takes on a constant value, one can see from Figure 6 (b) that  $\log \Gamma$  is almost proportional to  $\log \delta^{-2/3}$  for large  $\delta$ , and  $\log \Gamma$  increases and saturates to a constant as  $\delta$  decreases to a sufficiently small value. We note that a similar saturation effect in pre-bifurcation amplification was previously observed by Kravtsov and Surovyatkina [13] and Surovyatkina [14], who considered random noise in a one-dimensional map as  $\mu$  is varied to approach  $\mu_{\text{bif}}$ . Although the saturation of the gain is a universal property of dynamical systems, we note that it is very difficult to observe experimentally such phenomenon on paced cardiac tissues because of the existence of noise and the limitation on measurement resolution.

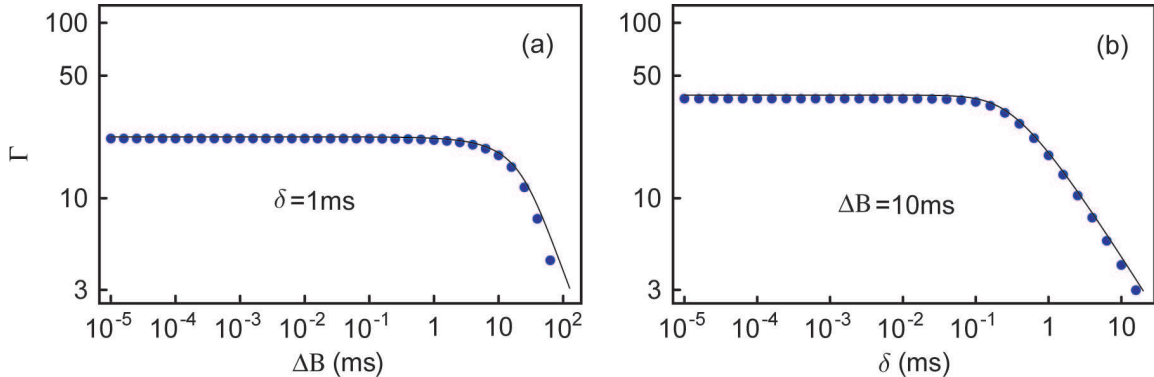


Figure 6: Saturation of the amplification gain in the two-dimensional cardiac map illustrated by (a)  $\log \Gamma$  vs.  $\log \Delta B$ , where  $\Delta B = B - B_{\text{bif}}$  and (b)  $\log \Gamma$  vs.  $\log a$ : the solid curves correspond to results from the higher-order analysis and the dots correspond to numerical simulations.

Because pre-bifurcation amplification is a property of the period-doubling bifurcation, its observable region in terms of the control parameter and the perturbation amplitude is problem-dependent and limited in parameter space to a vicinity of the bifurcation point. Under some circumstances, de-amplification gains (gains less than 1) may be obtained for a control parameter  $\mu$  sufficiently far away from  $\mu_{\text{bif}}$ . Moreover, other responses rather than the presumed period-two solutions may also exist. For example, as shown in Fig. 7, a period-doubling cascade to chaos is observed in the two-dimensional cardiac model under increase of the perturbation amplitude  $\delta$ . These observations suggest that caution should be taken when using pre-bifurcation amplification as a technique to detect the existence of period-doubling bifurcations.

### Acknowledgments

Support of the National Institutes of Health under grant 1R01-HL-72831 and the National Science Foundation under grants DMS-9983320 and PHY-0243584 is gratefully acknowledged.

### References

- [1] J. Heldstab, H. Thomas, T. Geisel, and G. Randons, ‘Linear and Nonlinear Response of Discrete Dynamical Systems I. Periodic Attractors,’ *Z. Phys. B* **50**, 141-150 (1983).
- [2] A. Arneodo, ‘Scaling for a Periodic Forcing of a Period-Doubling System,’ *Phys. Rev. Lett.* **53**, 1240; **54**, 86 (1984).

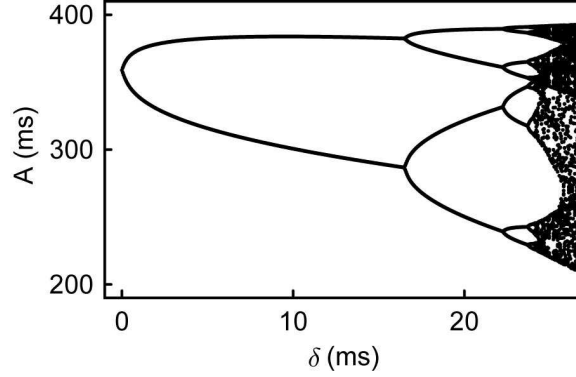


Figure 7: Variation of perturbed response under changes in perturbation amplitude  $\delta$  for the two-dimensional cardiac map described in Eqs. (55) and (56). Here, the control parameter is chosen to be  $B = B_{\text{bif}} + 10$  ms.

- [3] F. Argoul, A. Arneodo, O. Richetti, J.C. Roux, and H.L. Swinney, 'Transitions to Chaos in the Presence of an External Periodic Field - Crossover Effect in the Measure of Critical Exponents,' *Europhys. Lett.* **3**, 643 (1987).
- [4] S.P. Kuznetsov, 'Effect of a Periodic External Perturbation on a System which Exhibits an Order-Chaos Transition through Period-Doubling Bifurcation,' *JETP Lett.* **39**, 133 (1984).
- [5] S.P. Kuznetsov and A.S. Pikovsky, 'Renormalization Group for the Response Function and Spectrum of the Period-Doubling System,' *Phys. Lett. A* **94**, 1 (1989).
- [6] N.Yu. Ivan'Kov and S.P. Kuznetsov, 'Different Types of Scaling in the Dynamics of Period-Doubling Maps under External Periodic Driving,' *Discrete Dynamics in Nature and Society* **5**, 223 (2000).
- [7] K. Wiesenfeld, 'Virtual Hopf phenomenon: A new precursor of period-doubling bifurcations,' *Phys. Rev. A* **32**, 1744 (1985).
- [8] K. Wiesenfeld and B. McNamara, 'Small-signal amplification in bifurcating dynamical systems,' *Phys. Rev. A* **33**, 629-642 (1986); erratum: *ibid* **33**, 3578 (1986).
- [9] P. Bryant and K. Wiesenfeld, 'Suppression of Period-Doubling and Nonlinear Parametric Effects in Periodically Perturbed Systems,' *Phys. Rev. A* **33**, 2525 (1986).
- [10] H. Svensmark and K. Wiesenfeld, 'Scaling Law for the Idler near a Bifurcation,' *Phys. Rev. A* **46**, 787 (1992).
- [11] S.T. Vohra, F. Bucholtz, K.P. Koo, and D.M. Dagenais, 'Experimental Observation of Period-Doubling Suppression in the Strain Dynamics of a Magnetostrictive Ribbon,' *Phys. Rev. Lett.* **66**, 212 (1991).
- [12] S.T. Vohra and K. Wiesenfeld, 'Experimental Test of the Normal Form for Period Doubling Bifurcations,' *Physica D* **86**, 27 (1995).
- [13] Yu. A. Kravtsov and E.D. Surovyatkina, 'Nonlinear saturation of prebifurcation noise amplification,' *Phys. Lett. A* **319**, 348 (2003).
- [14] E.D. Surovyatkina, 'Rise and saturation of the correlation time near bifurcation threshold,' *Phys. Lett. A* **329**, 169 (2004).
- [15] D.R. Chialvo, D.C. Michaels, and J. Jalife, 'Supernormal excitability as a mechanism of chaotic dynamics of activation in cardiac Purkinje fibers,' *Circ. Res.* **66**, 525-545 (1990).
- [16] G.M. Hall and D.J. Gauthier, 'Experimental control of cardiac muscle alternans,' *Phys. Rev. Lett.* **88**, 198102 (2002).

- [17] J.J. Fox, E. Bodenschatz, and R.F. Gilmour, Jr., 'Period-doubling instability and memory in cardiac tissue,' *Phys. Rev. Lett.* **89**, 138101 (2002).
- [18] C.M. Berger, H. Dobrovolny, X. Zhao, D.G. Schaeffer, W. Krassowska, and D.J. Gauthier, 'Investigating a Period-Doubling Bifurcation in Cardiac Tissue Using Alternate Pacing,' *Dynamics Days*, Bethesda, MD, January 4-7, 2006
- [19] American Heart Association: Heart Disease and Stroke Statistics - 2004 Update. American Heart Association, Dallas, TX, 2004.